

1 Spatial Order in Liquid Crystals: Computer Simulations of Systems of Ellipsoids

Friederike Schmid and Nguyen H. Phuong

Theoretische Physik, Universität Bielefeld, D-33501 Bielefeld, Germany

Abstract. Computer simulations of simple model systems for liquid crystals are briefly reviewed, with special emphasis on systems of ellipsoids. First, we give an overview over some of the most commonly studied systems (ellipsoids, Gay-Berne particles, spherocylinders). Then we discuss the structure of the nematic phase in the bulk and at interfaces.

1.1 Introduction

Randomly distributed hard spheres in three dimensions form two types of structures, depending on their density: Fluid and crystalline. For randomly distributed anisotropic particles, the situation can be different: Several phases may exist at intermediate densities between the fluid and the solid state. These phases are called "mesophases". For example, one often observes a nematic phase where the particles are oriented in one common preferred direction, but have no crystalline translational order. Other common phases are the smectic phases, in which the particles are arranged in layers of two dimensional fluids. Some of these structures are sketched in Figure 1. Since the mesophases are neither crystalline nor truly liquid, they are commonly referred to as "liquid crystal phases".

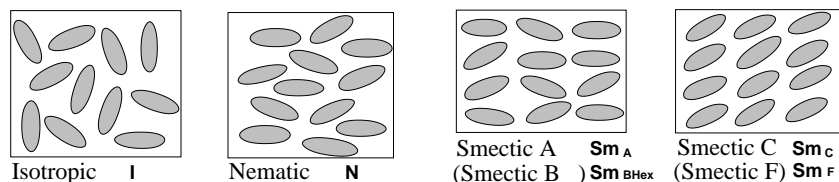


Figure 1:

Liquid crystalline phases. In the Smectic B_{Hex} and Smectic F phase, the structure within the layers is not entirely fluid, but has a type of order called hexatic. See Ref. [1,2] for explanation.

Experimentally, such phases are observed in various systems of anisotropic particles: Small organic molecules, stiff polymers, self-associated wormlike micelles, or

even whole viruses (one famous example being the tobacco mosaic virus). The phase transitions are triggered in some cases by the temperature (thermotropic liquid crystals), and in other cases by the concentration of the anisotropic particles (lyotropic liquid crystals). In reality, particles are of course not distributed "randomly", but according to a Boltzmann distribution $P \propto e^{-E/k_B T}$ which accounts for the energy E of their mutual interactions (T is the temperature and k_B the Boltzmann constant). Nevertheless, the mechanisms which drive the phase transitions in lyotropic liquid crystals are essentially the same as those in systems of hard anisotropic particles. Therefore, the latter are often employed to model phase transitions in liquid crystals. More generally, systems of anisotropic particles with simplified interactions have proven very useful to study generic properties of liquid crystals [1,3,4,5,6].

In the present contribution, we describe some of the computer simulation work that has been done in this direction. We do not intend to give a complete account of this active and rapidly progressing field of research. The limited space here permits only a rather crude introduction and the discussion of a few examples. The reader who is interested in more exhaustive overviews is referred to, e.g., the set of review articles in Ref. [6], or to Refs. [5,7,8].

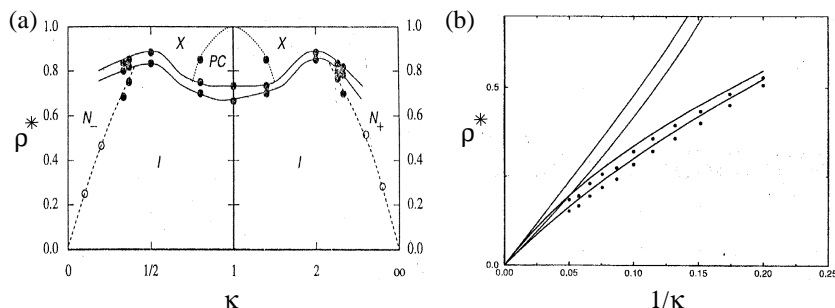
The paper is organized as follows: First, we review some of the most commonly studied idealized models for particle based simulations. We will then focus on the nematic phase and discuss some of its bulk properties. Finally, we address specific issues of interfacial properties in nematic liquid crystals.

1.2 Model systems

1.2.1 Ellipsoids

Perhaps the most obvious anisotropic generalization of hard spheres are hard ellipsoids of revolution with one symmetry axis of length L and transverse thickness D . The phase diagram in three dimensions has been established from computer simulations by Frenkel, Allen and coworkers [9,10,11,12,13,14]. It is shown for a range of elongations $\kappa = L/D$ in Figure 2. If the particles are sufficiently anisotropic, a nematic phase (N) intrudes between the isotropic (I) and the crystalline (X,PC) phase. No further liquid crystalline phases are present. In particular, smectic phases do not exist. This makes hard ellipsoids particularly suited to study the properties of nematic liquid crystals.

From a technical point of view, the study of ellipsoids is complicated by the fact that the contact distance $\sigma(\mathbf{u}_i, \mathbf{u}_j, \hat{\mathbf{r}}_{ij})$ between two particles i and j with orientations \mathbf{u}_i and \mathbf{u}_j in the center-center direction $\hat{\mathbf{r}}_{ij}$ ($|\mathbf{u}_{i,j}| = |\hat{\mathbf{r}}_{ij}| = 1$) cannot be given in analytically closed form. Criteria to decide whether or not two particles overlap have been derived by Vieillard-Baron [16], and by Perram and Wertheim [17,18]. Technical details on the implementation can be found in the review article Ref. [11].


Figure 2:

Phase diagram of hard ellipsoids as a function of elongation $\kappa = L/D$ and reduced density ρ/ρ_{cp} (ρ_{cp} being the density at hcp packing). Phases are: I (isotropic phase), N (nematic phase), X (orientationally ordered crystalline phase), PC (orientationally disordered crystalline phase). (a) Full range of elongations: From Ref. [5], with data from Refs. [9,10,12,15]. (b) Detail from Ref. [14]. Points denote simulation data, lines predictions from different theories.

Both the simulation and the data analysis are simplified considerably if an explicit formula for $\sigma(\mathbf{u}_i, \mathbf{u}_j, \hat{\mathbf{r}}_{ij})$ is available. For this reason, Berne and Pechukas [19] have proposed an approximate expression

$$\sigma(\mathbf{u}_i, \mathbf{u}_j, \hat{\mathbf{r}}_{ij}) = \sigma_0 \left\{ 1 - \frac{\chi}{2} \left[\frac{(\mathbf{u}_i \cdot \hat{\mathbf{r}}_{ij} + \mathbf{u}_j \cdot \hat{\mathbf{r}}_{ij})^2}{1 + \chi \mathbf{u}_i \cdot \mathbf{u}_j} + \frac{(\mathbf{u}_i \cdot \hat{\mathbf{r}}_{ij} - \mathbf{u}_j \cdot \hat{\mathbf{r}}_{ij})^2}{1 - \chi \mathbf{u}_i \cdot \mathbf{u}_j} \right] \right\}^{-1/2}, \quad (1.1)$$

with the anisotropy parameter $\chi = (\kappa^2 - 1)/(\kappa^2 + 1)$. This function gives the exact contact distance if the particles i and j are co-linear (parallel to each other), and overestimates it by a factor of at most $\sqrt{2}/\sqrt{1 + 2\kappa/(\kappa^2 + 1)} < \sqrt{2}$ otherwise. A few simulation studies have considered systems of “hard” particles with contact distances given by Eqn. (1.1) (“hard Gaussian overlap particles”) [20,21,22,23,24,25]. Much more commonly, however, the contact function (1.1) is used in conjunction with Lennard-Jones type interaction potentials, the Gay-Berne potential [26]. This class of models will be discussed in the next section. The present authors favor yet another potential, which is purely repulsive but soft.

$$V_{ij} = \begin{cases} 4\epsilon_0 (R_{ij}^{-12} - R_{ij}^{-6}) + \epsilon_0, & R_{ij}^{-6} < 2 \\ 0, & \text{otherwise} \end{cases}, \quad (1.2)$$

where R_{ij} is a reduced distance,

$$R_{ij} = (r_{ij} - \sigma(\mathbf{u}_i, \mathbf{u}_j, \hat{\mathbf{r}}_{ij}) + \sigma_0)/\sigma_0 \quad (1.3)$$

As far as we have seen so far, systems of such “soft ellipsoids” (at temperature $k_B T \sim \epsilon$) have almost the same structure as systems of hard ellipsoids.

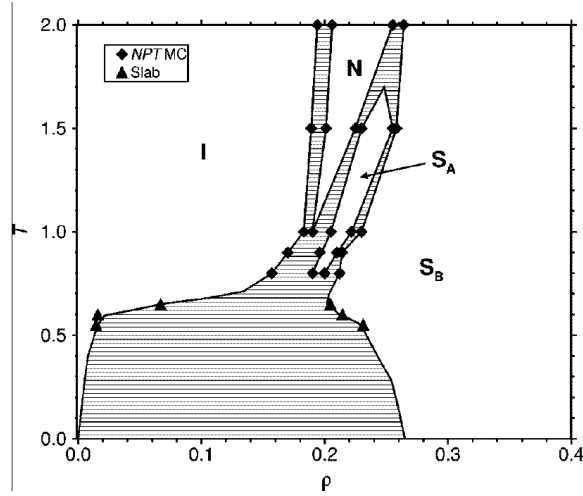


Figure 3:

Phase diagram of Gay-Berne ellipsoids with $\mu = 2$, $\nu = 1$, $\kappa = 4$, and $\kappa' = 5$ as a function of temperature T in units of ϵ_0/k_B and number density ρ . In addition to the phases observed for hard ellipsoids (Figure 2), one also finds smectic phases S_A and S_B . The simulations did not allow to decide whether the smectic B phase is hexatic or solid, i.e., crystalline. In the smectic A phase, however, the smectic layers are undoubtedly fluid. From Ref. [32]

1.2.2 Gay-Berne particles

Despite their appealing simplicity, hard or soft repulsive ellipsoids are not in every respect best suited to study generic liquid crystal properties. For example, such models do not exhibit smectic phases. Furthermore, one cannot study the effect of attractive interactions, the interplay between liquid-crystalline order and liquid-vapor phase separation etc. Therefore, Gay and Berne [26] have introduced a class of ellipsoidal pair potentials with attractive interactions, which has become one of the standard liquid crystal potentials.

The functional form of these potentials is

$$V_{ij} = 4 \epsilon_0 \epsilon'(\mathbf{u}_i, \mathbf{u}_j, \hat{\mathbf{r}}_{ij})^\mu \epsilon''(\mathbf{u}_i, \mathbf{u}_j)^\nu (R_{ij}^{-12} - R_{ij}^{-6}), \quad (1.4)$$

where the reduced distance R_{ij} defined is as above (eqn. (1.3) with σ taken from (1.1)), and the energy functions ϵ are given by

$$\epsilon'(\mathbf{u}_i, \mathbf{u}_j, \hat{\mathbf{r}}_{ij}) = 1 - \frac{\chi'}{2} \left[\frac{(\mathbf{u}_i \cdot \hat{\mathbf{r}}_{ij} + \mathbf{u}_j \cdot \hat{\mathbf{r}}_{ij})^2}{1 + \chi' \mathbf{u}_i \cdot \mathbf{u}_j} + \frac{(\mathbf{u}_i \cdot \hat{\mathbf{r}}_{ij} - \mathbf{u}_j \cdot \hat{\mathbf{r}}_{ij})^2}{1 - \chi' \mathbf{u}_i \cdot \mathbf{u}_j} \right] \quad (1.5)$$

$$\epsilon''(\mathbf{u}_i, \mathbf{u}_j) = [1 - \chi^2 (\mathbf{u}_i \cdot \mathbf{u}_j)^2]^{-1/2}. \quad (1.6)$$

The new additional anisotropy parameter χ' accounts for the fact that the attractive energy should favor a side-by-side alignment of particles compared to an end-to-end alignment. It is related to the corresponding ratio of minimum energies (well depths) $\kappa' = \epsilon_{\text{side-side}}/\epsilon_{\text{end-end}}$ via $\chi' = (\kappa'^{1/\mu} - 1)/(\kappa'^{1/\mu} + 1)$. Gay and Berne originally suggested to choose the exponents $\mu = 2$ and $\nu = 1$. The phase behavior for this set of exponents has been studied in detail [27,28,29,30,31,32], for various choices of κ and κ' [30,31,32]. An example is shown in Figure 3. One observes a liquid-vapor coexistence region at low temperature. Furthermore, the attractive interaction stabilizes a smectic phase (Sm A), which consists of stacked layers of two dimensional fluids.

The Gay-Berne model is widely used in liquid crystal simulations [6]. Due to the option of varying not only κ and κ' , but also the exponents μ and ν , it is very versatile [33,34]. Luckhurst et al have demonstrated that it can even be adjusted to serve as a good model for a real thermotropic liquid crystal [35,36].

1.2.3 Other models

Ellipsoids are not the only particles that have been used to model liquid crystals on an idealized level. An almost equal amount of work has been devoted to systems of spherocylinders: Cylinders of length L and diameter D capped with hemispheres at both ends. They have the advantage that the contact distance σ between two particles can be evaluated exactly [37]. Furthermore, they resemble quite closely certain real colloidal liquid crystal substances, e. g., rodlike viruses [38,39,40,41].

The phase behavior of hard spherocylinders has been studied by Frenkel and others [42,43,44,45,46,47]. The complete phase diagram for all elongations L/D as computed by Bolhuis and Frenkel [46] is shown in Figure 4. It differs strikingly from the corresponding phase diagram for hard ellipsoids in that sufficiently elongated spherocylinders form smectic phases. This came as a surprise when it was first discovered in simulations [42]. Meanwhile, it has been reproduced by density functional theories [48,49,50,51,52].

Bolhuis et al [53] have studied the influence of attractive interactions on the phase behavior of spherocylinders. Like in systems of Gay-Berne particles (Figure 3), a liquid-vapor coexistence region emerges at low temperatures (see also Ref. [54]). The influence of polydispersity – i. e., fluctuating rod length – on the phase diagram has been investigated by Bates et al [55]. Perhaps not surprisingly, the smectic phase is destabilized in favor of the nematic phase.

We shall only briefly mention some other particle based model systems for liquid crystals: In a number of studies, liquid crystalline molecules have been modeled by stiff chain molecules [56,57,58,59,60,61,62,63]. with aspect ratio $\kappa < 1$ and spheres cut at both sides have been used to study discotic liquid crystals, i. e., fluids of disklike particles [64,65,66,67,68,69]. Such fluids exhibit new, different types of liquid crystalline order. For example, the smectic phases are replaced

by columnar phases: The discs assemble into hexagonal arrays of columns, but remain fluid in one dimension within the columns.

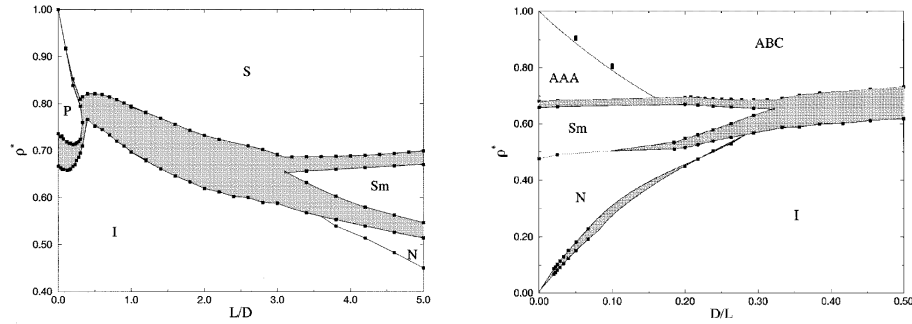


Figure 4:

Phase diagram of hard spherocylinders as a function of reduced density $\rho^* = \rho/\rho_{cp}$ and elongation L/D (left) or inverse elongation D/L (right). Phases are: I (isotropic phase), N (nematic phase), Sm (smectic A phase), AAA, S=ABC, (two types of solid phases with orientational order), and P (orientationally disordered solid phase). From Ref. [46]. The transition between the nematic and the smectic phase is first order at all elongations [47].

1.3 Properties of the nematic phase

A number of important properties of the nematic phase can already be deduced from very general considerations.

First, geometric arguments suggest that the transition between the isotropic and the nematic phase should be discontinuous or first order, i.e., there should be a density regime in which both phases coexist. This is a consequence of “Landau’s rule” [1,70], which relates the character of the phase transition to the symmetry groups of the two phases. Landau’s rule is not rigorous, it does not exclude the possibility that the width of the coexistence region may happen to shrink to zero in certain points of the phase diagram. Moreover, order fluctuations may affect the nature of the phase transition. So far, however, the actually observed isotropic-nematic transitions have been discontinuous, albeit with rather narrow coexistence regions.

Second, the free energy cost of spatial modulations of the average particle orientation must vanish if the wavelength of the modulations tends to infinity. This is an example of Goldstone’s theorem [71,72]: If the order parameter in an ordered phase breaks a continuous symmetry, there exist soft massless fluctuation modes [73]. Modulations with finite wavelength are subject to elastic

restoring forces [73,74]. For symmetry reasons, these depend on only three material constants, the Frank elastic constants K_{11}, K_{22}, K_{33} [75,76,77]. Figure 5 illustrates the corresponding fundamental distortions, the “splay”, “twist” and “bend” mode.

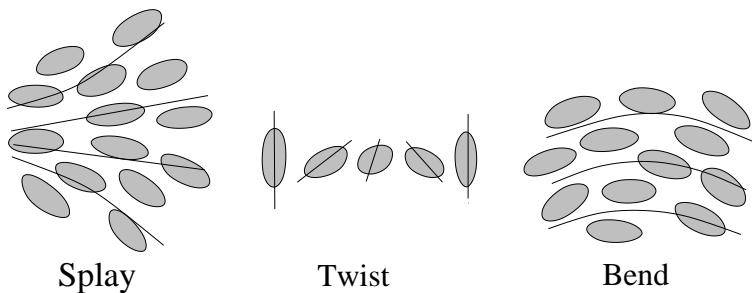


Figure 5:
Elastic modes in nematic liquid crystals.

We turn to give a more quantitative description. The nematic order is usually characterized by the 3×3 dimensional nematic order tensor [1]

$$\mathbf{Q} = \frac{1}{N} \sum_{i=1}^N \left(\frac{3}{2} \mathbf{u}_i \otimes \mathbf{u}_i - \frac{1}{2} \mathbf{1} \right), \quad (1.7)$$

where the sum runs over all particles i , $\mathbf{1}$ denotes the unit matrix and \otimes the dyadic product. The largest eigenvalue of \mathbf{Q} is the nematic order parameter per particle, and the corresponding eigenvector is the director \mathbf{n} of the nematic liquid. It gives the direction of preferential alignment of the molecules. Long wavelength spatial modulations $\mathbf{n}(\mathbf{r})$ of the director are penalized by the elastic free energy [77]

$$\mathcal{F}\{\mathbf{n}(\mathbf{r})\} = \frac{1}{2} \int d\mathbf{r} \left\{ K_{11} [\nabla \cdot \mathbf{n}]^2 + K_{22} [\mathbf{n} \cdot (\nabla \times \mathbf{n})]^2 + K_{33} [\mathbf{n} \times (\nabla \times \mathbf{n})]^2 \right\}. \quad (1.8)$$

On macroscopic length scales, the structure of liquid crystals is controlled almost exclusively by the elastic energy and thus by the Frank elastic constants K_{11} , K_{22} , and K_{33} .

The quantitative characterization of the local, microscopic structure is much more involved. The most intensely studied quantities are usually the pair distributions or the pair correlation functions. On principle, a hierarchy of infinitely many N -particle distribution functions would be required to fully characterize a fluid. In systems with only pairwise interactions, however, the pair distributions stand out because they can be used to calculate several macroscopic quantities such as the pressure and the compressibility. Moreover, pair correlations are often accessible to experiments in real systems.

As before, we characterize the orientation of a particle by a unit vector \mathbf{u} . The one-particle distribution $\rho^{(1)}(\mathbf{u}, \mathbf{r})$ gives the probability density of finding a particle of orientation \mathbf{u} at the position \mathbf{r} . Similarly, the two-particle distribution $\rho^{(2)}(\mathbf{u}_i, \mathbf{r}_i, \mathbf{u}_j, \mathbf{r}_j)$ is the probability density of finding simultaneously one particle of orientation \mathbf{u}_i at the position \mathbf{r}_i , and another with orientation \mathbf{u}_j at the position \mathbf{r}_j . In a homogeneous nematic phase, $\rho^{(1)}$ does not depend on the position \mathbf{r} , and $\rho^{(2)}$ depends only on the relative position $\mathbf{r}_{ij} = \mathbf{r}_i - \mathbf{r}_j$. Furthermore, particles at infinite distances are uncorrelated, hence

$$\rho^{(2)}(\mathbf{u}_i, \mathbf{u}_j, \mathbf{r}) \xrightarrow{r \rightarrow \infty} \rho^{(1)}(\mathbf{u}_i) \rho^{(1)}(\mathbf{u}_j). \quad (1.9)$$

The correlations between particles at finite distance are characterized by the total correlation function [78,79]

$$h(\mathbf{u}_1, \mathbf{u}_2, \mathbf{r}) = \frac{\rho^{(2)}(\mathbf{u}_1, \mathbf{u}_2, \mathbf{r})}{\rho^{(1)}(\mathbf{u}_1) \rho^{(1)}(\mathbf{u}_2)} - 1, \quad (1.10)$$

It subsumes the total effect of a particle i on a particle j . Due to the elastic interactions mentioned above, it decays only slowly at long distances with the algebraic power law $1/r$.

Of course, other definitions of correlation functions are possible. As an alternative to the total correlation function, one could consider the orientation correlation function defined by Penttinen and Stoyan [80]. It describes the pure orientation correlations between particles at a given distance, and should display the same asymptotic $1/r$ power law in the nematic fluid as h .

The long range correlations are mediated by the whole bulk of the surrounding nematic fluid. It seems desirable to separate these “indirect” effects from a more local “direct” effect of two particles on each other. This can be done by considering the “direct correlation function” $c(\mathbf{u}_i, \mathbf{u}_j, \mathbf{r}_{ij})$, which is defined through the Ornstein-Zernike equation [78,79]

$$h(\mathbf{u}_i, \mathbf{u}_j, \mathbf{r}_{ij}) = c(\mathbf{u}_i, \mathbf{u}_j, \mathbf{r}_{ij}) + \int c(\mathbf{u}_i, \mathbf{u}_k, \mathbf{r}_{ik}) \rho^{(1)}(\mathbf{u}_k) h(\mathbf{u}_k, \mathbf{u}_j, \mathbf{r}_{kj}) d\mathbf{u}_k d\mathbf{r}_k. \quad (1.11)$$

As it turns out, the direct correlation function is indeed short range even in the nematic phase.

We illustrate this with recent computer simulation results. We have performed computer simulations of 1000-8000 ellipsoids with elongation $\kappa = 3$ at the number density $\rho = 0.3$, interacting with the potential (1.2) at temperature $T = 0.5$. Technical details can be found in Refs. [81,83,84].

The calculation of direct correlation functions from computer simulations is computationally demanding and involves a complicated data analysis. We were the first to determine the direct correlation function from computer simulations of a nematic fluid without any approximations. Direct correlation functions in

isotropic fluids have been calculated earlier by Allen et al [85,86], and approximate data for nematic fluids have been derived from simulations by Stelzer et al [87,88].

Figure 6 shows the orientational average of the total correlation function and the direct correlation function. The average is carried out over the orientations \mathbf{u}_i , \mathbf{u}_j , and $\hat{\mathbf{r}}_{ij}$. Figure 6 demonstrates that long range algebraic correlations between particles are not apparent in this averaged curve. The elastic interactions affect only orientations, not total densities. Therefore, both h and c are short range.

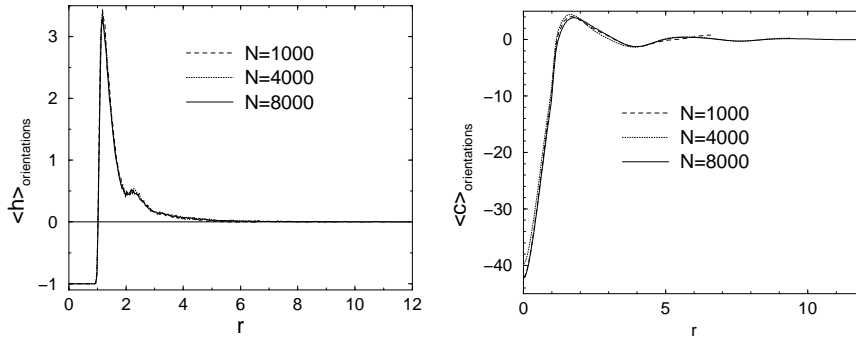


Figure 6:

Total correlation function h (left) and direct correlation function c (right) vs. molecular distance r , averaged over all orientations of $\mathbf{u}_i, \mathbf{u}_j$, and \mathbf{r}_{ij} , for different system sizes N .

In order to assess the effect of the elasticity, we need to study orientational dependent correlations. To this end, we expand all correlation functions in spherical harmonics $Y_{lm}(\mathbf{u})$.

$$F(\mathbf{u}_i, \mathbf{u}_j, \mathbf{r}) = \sum_{\substack{l_1, l_2, l \\ m_1, m_2, m}} F_{l_1 m_1 l_2 m_2 l m}(r) Y_{l_1 m_1}(\mathbf{u}_i) Y_{l_2 m_2}(\mathbf{u}_j) Y_{lm}(\hat{\mathbf{r}}), \quad (1.12)$$

where F stands for $\rho^{(2)}$, h , or c . The z axis is chosen in the direction of the director. The orientation dependence of the correlations is reflected by the coefficients with nonzero indices. Figure 7 (left) shows a coefficient of the total correlation function with a particularly pronounced long range tail. As shown in Figure 7 (right), the tail completely disappears in the direct correlation function.

The direct correlation function is a central quantity in theories of liquid matter [78]. It enters density functional theories which predict the structure of inhomogeneous fluids, e. g., fluids at interfaces. It allows to calculate a number of material constants of fluids. In nematic fluids, for example, it can be used to calculate the Frank elastic constants according to a set of equations first derived by Poniewierski and Stecki [89,90]. We have applied these equations to our

data and obtained a set of values for K_{11} , K_{22} , and K_{33} , which is in agreement with results from a different, more direct method [81,82]. Thus the direct correlation function establishes a bridge between the microscopic structure and the parameters which characterize the macroscopic structure.

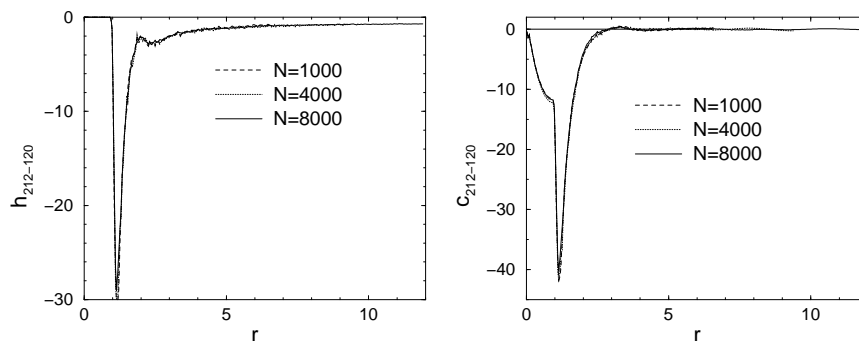


Figure 7:

Expansion coefficient with $l_1 = 2, l_2 = 2, m_1 = 1, m_2 = -1, l = 2$, and $m = 0$ of the total correlation function h (left), and the direct correlation function (right) vs. molecular distance r for different system sizes N . Left Figure: Dashed line indicates an extrapolation with a $1/r$ power law behavior. Inset shows the same data vs. $1/r$.

1.4 Interfacial properties

We turn to discuss briefly the interfacial properties in nematic liquid crystals. These are of great interest in the liquid crystal display technology [91]. Therefore, a growing number of simulations are devoted to the study of model nematics at surfaces [93,94,95,96,97,98,99,100,101,102,103,104,105,106,107]. and interfaces [108,109,110,111,112] or in thin films [24,25,113,114,115,116,117,118].

The microscopic structure at surfaces can be quite complex [93,94,95,96]. From a macroscopic point of view, the presence of surfaces or interfaces introduces essentially three new effective parameters: the interfacial tension, the anchoring angle, and the anchoring energy. The anchoring angle is the angle with respect to the surface which the director preferably assumes close to the surface. The anchoring energy is related to the force needed to twist the director out of the anchoring angle.

The anchoring angle can be calculated from simulations in a straightforward way. Obtaining the anchoring energy is more difficult and time consuming. Allen and coworkers have devised different methods and applied them to systems of ellipsoids at hard, planar walls [106,107]. The interfacial tension can be computed from the anisotropy of the pressure tensor close to the surface [111,119], or in the case of fluid-fluid interfaces from their undulations (capillary waves) [112].

Recently, a number studies have been devoted to the interface between the nematic and the isotropic phase in Gay-Berne fluids [108] and fluids of spherocylinders [110] or ellipsoids [109,111,112]. They reveal among other a rather intriguing capillary wave spectrum. It reflects a complex interplay between the bare surface tension and the elastic interactions in the nematic phase [112].

1.5 Conclusions

In materials science, systems of ellipsoids serve as model systems which exhibit generic properties of nematic liquid crystals. They are studied for the general insight they can give into the physics of liquid crystals, and also because simulations of ellipsoids are computationally much cheaper than simulations of a comparable number of more realistic molecules. However, fluids of ellipsoids are also fascinating from a much more general point of view: They are simple systems where purely entropic effects generate an amazing variety of different structures, and lead to unusual long-range static and dynamic properties. Computer simulations are often the only way of investigating some of that behavior.

Acknowledgements

We have benefitted from discussions and interactions with N. Akino, M. P. Allen, K. Binder, G. Germano, and H. Lange. N. H. P. acknowledges financial support by the German Science Foundation (DFG). The computer simulations of our group are carried out mostly on the CRAY T3Es of the NIC in Jülich.

References

1. De Gennes P. G. (1995): *The Physics of Liquid Crystals*. (Oxford University Press, Oxford)
2. Chandrasekhar, S. (1992): *Liquid Crystals*. (Cambridge University Press, Cambridge)
3. Onsager L. (1949): ‘The effects of shape on the interaction of colloidal particles’. *Ann. N.Y. Acad. Sci.* **51**, pp. 627–659.
4. Maier W., A. Saupe (1958): ‘Eine einfache molekulare Theorie des nematischen kristallin-flüssigen Zustandes’. *Z. Naturforschung* **A13**, 564–566.
5. Allen M. P. (1995): ‘Simulations and phase behaviour of liquid crystals’. In: *Observation, Prediction and Simulation of Phase Transitions in Complex Fluids*, ed. by M. Baus et al (Kluwer Academic Publ., Dordrecht), pp. 557–590.
6. Pasini P., C. Zannoni eds. (1998): *Advances in the Computer Simulations of Liquid Crystals*. (Kluwer Academic Publ., Dordrecht)
7. Crain J., A. V. Komolkin (1999): ‘Simulating molecular properties of liquid crystals’. *Adv. Chem. Phys.* **109**, 39–113.

8. Singh S. (2000): ‘Phase transitions in liquid crystals’. *Phys. Rep.* **324**, 108–269.
9. Frenkel D., B. M. Mulder (1985): ‘The hard ellipsoid-of-revolution fluid. I. Monte Carlo simulations’. *Molecular Physics* **55**, 1171–92.
10. Allen M. P., M. R. Wilson (1989): ‘Computer simulation of liquid crystals’. *Journal of Computer Aided Molecular Design* **3**, 335–353.
11. Allen M. P., G. T. Evans, D. Frenkel, B. Mulder (1993): ‘Hard convex body fluids’. *Adv. Chem. Phys.* **86**, 1–166.
12. Samborski A., G. T. Evans, C. P. Mason, M. P. Allen (1994): ‘The isotropic to nematic liquid crystal transition for hard ellipsoids: An Onsager-like theory and computer simulations’. *Molecular Physics* **81**, 263–76.
13. Allen M. P., C. P. Mason (1995): ‘Stability of the nematic phase for the hard ellipsoid fluid’. *Molecular Physics* **86**, 467–74.
14. Camp. P. J., C. P. Mason, M. P. Allen, A. A. Khare, D. A. Kofke (1996): ‘The isotropic-nematic phase transition in uniaxial hard ellipsoid fluids: Coexistence data and the approach to the Onsager limit’. *J. Chem. Phys.* **105**, 2837–2949.
15. Frenkel D., A. J. C. Ladd (1984). ‘New Monte Carlo method to compute the free energy of arbitrary solids. Application to the FCC and HCP phases of hard spheres’. *J. Chem. Phys.* **81**, 3188–93.
16. Vieillard-Baron J. (1972): ‘Phase transitions of the classical hard-ellipse system’. *J. Chem. Phys.* **56**, 4729–4744.
17. Perram J. W., M. S. Wertheim, J. L. Lebowitz, G. O. Williams (1984): ‘Monte Carlo simulation of hard spheroids’. *Chem. Phys. Lett.* **105**, 277–280.
18. Perram J. W., M. S. Wertheim (1985): ‘Statistical mechanics of hard ellipsoids. I. Overlap algorithm and the contact function’. *J. Comp. Phys.* **58**, 409–416.
19. Berne J. B., P. Pechukas (1971): ‘Gaussian model potentials for molecular interactions’. *J. Chem. Phys.* **56**, 4213–4216.
20. Rigby M. (1989): ‘Hard gaussian overlap fluids’. *Mol. Phys.* **68**, 687–697.
21. Padilla P., E. Velasco (1997): ‘The isotropic-nematic transition for the hard Gaussian overlap fluid: Testing the decoupling approximation’. *J. Chem. Phys.* **106**, 10299–10310.
22. Velasco E., P. Padilla (1998): ‘Nematic virial coefficients of very long hard molecules and Onsager theory’. *Mol. Phys.* **94**, 335–339.
23. Huang S. L., V. R. Bhetanabotla (1999): ‘Virial coefficients for the Hard Gaussian Overlap model’. *Int. J. Mod. Phys. C* **10**, 361–374 (1999).
24. Cleaver D. J., P. I. C. Teixeira (2001): ‘Discontinuous structural transition in a thin hybrid liquid crystal film’. *Chem. Phys. Lett.* **338**, 1–6.
25. Chrzanowska A., P. I. C. Teixeira, H. Ehrentraut, D. J. Cleaver (2001): ‘Ordering of hard particles between hard walls’. *J. Phys. - Cond. Matt.* **13**, 4715–4726.
26. Gay J. G., B. J. Berne (1980): ‘Modification of the overlap potential to mimic a linear site-site potential’. *J. Chem. Phys.* **74**, 3316–3319.
27. Adams D. J., G. R. Luckhurst, R. W. Phippen (1987): ‘Computer simulation studies of anisotropic systems. XVII. The Gay-Berne model nematogen’. *Mol. Phys.* **61** 1575–1580.
28. De Miguel E., L. F. Rull, M. K. Chalam, K. E. Gubbins, F. Van Swol (1991): ‘Location of the isotropic-nematic transition in the Gay-Berne model’. *Mol. Phys.* **72** 593–605.
29. de Miguel E., L. F. Rull, M. K. Chalam, K. E. Gubbins (1991): ‘Liquid crystal phase diagram of the Gay-Berne fluid’. *Mol. Phys.* **74**, 405–424.
30. Emsley J. W., G. R. Luckhurst, W. E. Palke, D. J. Tildesley (1992): ‘Computer simulation studies of the dependence on density of the orientational order in nematic liquid crystals’. *Liquid Crystals* **11**, 519–530.

31. de Miguel E., E. Martin del Rio, J. T. Brown, M. P. Allen (1996): ‘Effect of the attractive interactions on the phase behavior of the Gay-Berne liquid crystal model’. *J. Chem. Phys.* **105**, 4234–4249.
32. Brown J. T., M. P. Allen, E. Martin del Rio, E. de Miguel (1997): ‘Effects of elongation on the phase behavior of the Gay-Berne fluid’. *Phys. Rev. E* **57**, 6685–6699.
33. Luckhurst G. R., R. A. Stephens, R. W. Phippen (1990): ‘Computer simulation studies of anisotropic systems. XIX. Mesophases formed by the Gay-Berne model mesogen’. *Liquid Crystals* **8**, 451–464.
34. Berardi R., A. P. J. Emerson, C. Zannoni (1993): ‘Monte-Carlo investigations of a Gay-Berne liquid crystal’. *J. Chem. Soc. Faraday T.* **89**, 4069–4078.
35. Luckhurst G. R., P. S. J. Simmonds (1993): ‘Computer simulation studies of anisotropic systems. XXI. Parametrization of the Gay-Berne potential for model mesogens’. *Mol. Phys.* **80**, 233–252.
36. Bates M. A., G. R. Luckhurst (1999): ‘Computer simulation studies of anisotropic systems. XXX. The phase behavior and structure of a Gay-Berne mesogen’. *J. Chem. Phys.* **110**, 7087–7108.
37. Vieillard-Baron J. (1974): ‘The equation of state of a system of hard spherocylinders’. *Mol. Phys.* **28**, 809–818.
38. Zasadzinski J. A. N., M. J. Sammon, R. B. Meyer, M. Cahoon, D. L. D. Caspar (1986): ‘Freeze-fracture imaging of ordered phases of tobacco mosaic virus in water’. *Mol. Cryst. Liq. Cryst.* **138**, 211–229.
39. Zasadzinski J. A. N., R. B. Meyer (1986): ‘Molecular imaging of tobacco mosaic virus lyotropic nematic phases’. *Phys. Rev. Lett.* **56**, 636–6388.
40. Oldenbourg R., X. Wen, R. B. Meyer, D. L. D. Caspar (1988): ‘Orientational distribution function in nematic tobacco-mosaic-virus liquid crystals measured by X-ray diffraction’. *Phys. Rev. Lett.* **61**, 1851–1854.
41. Dogic Z., S. Fraden (1997): ‘Smectic phase in a colloidal suspension of semiflexible virus particles’. *Phys. Rev. Lett.* **78**, 2417–2420.
42. Frenkel D. (1987): ‘Onsager’s spherocylinders revisited’. *J. Phys. Chem.* **91**, 4912–4916.
43. Frenkel D., H. N. W. Lekkerkerker, A. Stroobants (1988): ‘Thermodynamic stability of a smectic phase in a system of hard rods’. *Nature* **332**, 822–823.
44. Veerman J. A. C., D. Frenkel (1990): ‘Phase diagram of a system of hard spherocylinders by computer simulation’. *Phys. Rev. E* **41**, 3237–3244.
45. McGrother S. C., D. C. Williamson, G. Jackson (1996): ‘A re-examination of the phase diagram of hard spherocylinders’. *J. Chem. Phys.* **104**, 6755–6771.
46. Bolhuis P., D. Frenkel (1996): ‘Tracing the phase boundaries of hard spherocylinders’, *J. Chem. Phys.* **106**, 666–687.
47. Polson J. M., D. Frenkel (1997): ‘First-order nematic-smectic phase transition for hard spherocylinders in the limit of infinite aspect ratio’. *Phys. Rev. E* **56**, R6260–R6263.
48. Poniewierski A., R. Holyst (1988): ‘Density-functional theory for nematic and smectic-A ordering of hard spherocylinders’. *Phys. Rev. Lett.* **61**, 2461–2464.
49. Somoza A. M., P. Tarazona (1990): ‘Nematic and smectic liquid crystals of hard spherocylinders’. *Phys. Rev. E* **41**, 965–970.
50. Poniewierski A., T. J. Sluckin TJ (1991): ‘Phase diagram for a system of hard spherocylinders’. *Phys. Rev. E* **43**, 6837–6842.
51. Graf H., H. Löwen (1999): ‘Density functional theory for hard spherocylinders: phase transitions in the bulk and in the presence of external fields’. *J. Phys.: Cond. Matt.* **11**, 1435–1452.

52. Velasco E., L. Mederos, D. E. Sullivan (2000): ‘Density-functional theory of inhomogeneous systems of hard spherocylinders’. *Phys. Rev. D* **62**, 3708–3718.
53. Bolhuis P. G., A. Stroobants, D. Frenkel, H. N. W. Lekkerkerker (1997): ‘Numerical study of the phase behavior of rodlike colloids with attractive interactions’. *J. Chem. Phys.* **107**, 1551–1564.
54. Williamson D. C., F. del Rio (1998): ‘The isotropic-nematic phase transition in a fluid of square well spherocylinders’. *J. Chem. Phys.* **109**, 4675–4686.
55. Bates M. A., D. Frenkel (1998): ‘Influence of polydispersity on the phase behavior of colloidal liquid crystals: A Monte Carlo simulation study’. *J. Chem. Phys.* **109**, 6193–6198.
56. Wilson M. R. (1994): ‘Molecular dynamics simulation of semiflexible mesogens’. *Mol. Phys.* **81**, 675–690.
57. Levesque D., M. Mazars, J. J. Weis (1995): ‘Monte Carlo study of the thermodynamic stability of the nematic phase of a semiflexible liquid crystal model’. *J. Chem. Phys.* **103**, 3820–3831.
58. Mazars M., D. Levesque, J. J. Weis (1997): ‘Monte Carlo study of a semiflexible liquid crystal model: The smectic phase’. *J. Chem. Phys.* **106**, 6107–6115.
59. Affouard F., M. Kröger, S. Hess (1996): ‘Molecular dynamics of model liquid crystals composed of semiflexible molecules’. *Phys. Rev. E* **54**, 5178–5186.
60. Williamson D. C., G. Jackson (1998): ‘Liquid crystalline phase behavior in systems of hard-sphere chains’. *J. Chem. Phys.* **108**, 10294–10302.
61. Faller R., A. Kolb, F. Müller-Plathe (1999): ‘Local chain ordering in amorphous polymer melts: influence of chain stiffness’. *PCCP Phys. Chem. Chem. Phys.* **1**, 2071–2076.
62. Weber H., W. Paul, K. Binder (1999): ‘Monte Carlo simulation of a lyotropic first-order isotropic-nematic phase transition in a lattice polymer model’. *Phys. Rev. E* **59**, 2168–2174.
63. McBride C., C. Vega, L. G. MacDowell (2001): ‘Isotropic-nematic phase transition: Influence of intramolecular flexibility using a fused hard sphere model’. *Phys. Rev. E* **64**, 11703–11718.
64. Veerman J. A. C., D. Frenkel (1992): ‘Phase behavior of disklike hard-core mesogens’. *Phys. Rev. E* **45**, 5632–5648.
65. Bates M. A., G. R. Luckhurst (1996): ‘Computer simulation studies of anisotropic systems. XXVI Monte Carlo investigations of a Gay-Berne discotic at constant pressure’. *J. Chem. Phys.* **104**, 6696–6709.
66. De Luca M. D., M. K. Griffiths, C. M. Care, M. P. Neal (1994): ‘Computer modelling of discotic liquid crystals’. *Intl. J. Electr.* **77**, 907–917.
67. Emerson A. P. J., G. R. Luckhurst, S. G. Whatling (1994): ‘Computer simulation studies of anisotropic systems. XXIII. The Gay-Berne discogen’. *Mol. Phys.* **82**, 113–124.
68. Zewdie H. (1998): ‘Computer-simulation studies of diskotic liquid crystals’. *Phys. Rev. E* **57**, 1793–1805.
69. Bates M. A., D. Frenkel (1998): ‘Infinitely thin disks exhibit a first order nematic-columnar phase transition’. *Phys. Rev. E* **57**, 4824–4826.
70. Landau L. D., E. M. Lifschitz (1969): *Course of theoretical physics, Vol.5 Statistical physics*. (Pergamon Press Ltd. Oxford)
71. J. Goldstone J. (1961): ‘Field theories with ‘superconductor’ solutions’. *Nuovo Cimento* **19**, 154–164.
72. Goldstone J., A. Salam, S. Weinberg (1962). ‘Broken Symmetries’. *Phys. Rev.* **127**, 965–970.

73. Forster D. (1975): *Hydrodynamic Fluctuations, Broken Symmetry and Correlation Functions*. Vol. 47 of *Frontiers in Physics* (Benjamin, Reading, MA)
74. Chaikin, P. M., Lubensky, T. C. (1995): *Principles of condensed matter physics*. (Cambridge University Press, Cambridge)
75. Oseen, C. (1933): ‘The theory of liquid crystals’. *Trans. Faraday Soc.* **29**, 883–899.
76. Zöcher, H. (1933). *Trans. Faraday Soc.* **29**, 945–957.
77. Frank, F. C. (1958): ‘On the theory of liquid crystals’. *Discuss. Faraday Soc.* **25**, 19–29.
78. Hansen, J. P., I. R. McDonald (1986): *Theory of Simple Liquids*. (Academic Press, London, 1986).
79. Gray C. G., K. E. Gubbins (1984): *Theory of Molecular Fluids*, Vol. 1. (Oxford University Press, New York)
80. Penttinen A. K., D. Stoyan (1989): ‘Statistical analysis for a class of line segment processes’. *Scand. J. Statist* **16**, 153–168.
81. Phuong N. H., G. Germano, F. Schmid (2001): ‘Elastic constants from direct correlation functions in nematic liquid crystals: A computer simulation study’. *J. Chem. Phys.* **115**, 7227–7234 (2001).
82. Allen M. P., M. A. Warren, M. R. Wilson, A. Sauron, W. Smith (1997): ‘Molecular dynamics calculation of elastic constants in Gay-Berne nematic liquid crystals’. *J. Chem. Phys.* **105**, 2850–2858.
83. Phuong N. H., G. Germano, F. Schmid (2001): ‘The direct correlation function in nematic liquid crystals from computer simulation’. *Comp. Phys. Comm*, in print.
84. Phuong N. H., F. Schmid (2001): ‘Liquid structure of nematic and isotropic liquid crystals’. in preparation.
85. Allen M. P., C. P. Mason, E. de Miguel, J. Stelzer (1995): ‘Structure of molecular liquids’. *Phys. Rev. E* **52**, R25–R52.
86. Allen M. P., J. T. Brown, M. A. Warren (1996): ‘Computer simulation of liquid crystals’. *J. Phys.: Cond. Matt.* **8**, 9433–9437.
87. Stelzer J., L. Longa, H. R. Trebin (1995): ‘Molecular dynamics simulations of a Gay-Berne nematic liquid crystal – elastic properties from direct correlation functions.’ *J. Chem. Phys.* **103**, 3098–3107.
88. Stelzer J., L. Longa, H. R. Trebin (1995): ‘Elastic constants of nematic liquid crystals from molecular dynamics simulations’. *Mol. Cryst. Liq. Cryst. A* **262**, 455–461.
89. Poniewierski A., J. Stecki (1979): ‘Statistical theory of the elastic constants of nematic liquid crystals’. *Mol. Phys.* **38**, 1931–1940.
90. Poniewierski A., J. Stecki (1982): ‘Statistical theory of the Frank elastic constants’. *Phys. Rev. A* **25**, 2368–2370.
91. Bahadur B. (ed.) (1990): *Liquid crystals and uses* (World Scientific, Singapore)
92. Schadt M. (1997): ‘Liquid crystal materials and liquid crystal displays’. *Ann. Rev. Mater. Science*, **27**, 305–379.
93. Stelzer J., P. Galatola, G. Barbero G, L. Longa (1997): ‘Surface-induced order parameter profiles in a nematic liquid crystal from molecular dynamics simulations’. *Mol. Cryst. Liq. Cryst. A* **229**, 61–64.
94. Stelzer J., P. Galatola, G. Barbero, L. Longa (1997): ‘Molecular dynamics simulations of surface-induced ordering in a nematic liquid crystal’. *Phys. Rev. E* **55**, 477–480.
95. Stelzer J., L. Longa L, H. R. Trebin (1997): ‘Homeotropic surface anchoring of a Gay-Berne nematic liquid crystal’. *Phys. Rev. E* **55**, 7085–7089.
96. Palermo V., F. Biscarini, C. Zannoni (1998): ‘Abrupt orientational changes for liquid crystals adsorbed on a graphite surface’. *Phys. Rev. E* **57**, R2519–R2522.

97. Miyazaki T., K. Shigematsu, M. Yamashita (1998): ‘Surface-stabilized smectic A phase in the Gay-Berne model’. *J. Phys. Soc. Jpn* **67**, 3477–3487.
98. Miyazaki T., H. Hayashi, M. Yamashita (1999): ‘Surface-induced spatial ordering in nematic and smectic phases of Gay-Berne model’. *Mol. Cryst. Liq. Cryst. A* **330**, 1611–1618.
99. del Rio E. M., E. deMiguel (1997): ‘Computer simulation study of the free surfaces of a liquid crystal model’. *Phys. Rev. E* **55**, 2916–2924.
100. De Miguel E., E. M. Del Rio (1999): ‘Simulation of nematic free surfaces’. *Int. J. Mod. Phys. C* **10**, 431–433.
101. Doerr T. P., P. L. Taylor (1999): ‘Molecular dynamics simulations of liquid crystal anchoring at an amorphous polymer surface’. *Int. J. Mod. Phys. C* **10**, 415–429.
102. Doerr T. P., P. L. Taylor (1999): ‘Simulation of liquid crystal anchoring at an amorphous polymer surface from various initial configurations’. *Mol. Cryst. Liq. Cryst. A* **330**, 1735–1740 (1999).
103. Emerson A. P. J., S. Faetti, C. Zannoni (1997): ‘Monte Carlo simulation of the nematic-vapour interface for a Gay-Berne liquid crystal’. *Chem. Phys. Lett.* **271**, 241–246.
104. Binger D. R. , S. Hanna S (1999): ‘Computer simulation of interactions between liquid crystal molecules and polymer surfaces - I. Alignment of nematic and smectic A phases’. *Liqu. Cryst.* **26**, 12050–1224.
105. Xu J. L., R. L. B. Selinger, J. V. Selinger, R. Shashidar (2001): ‘Monte Carlo simulation of liquid-crystal alignment and chiral symmetry-breaking’. *J. Chem. Phys.* **115**, 4333–4338.
106. Allen M. P. (1999): ‘Molecular simulation and theory of liquid crystal surface anchoring’. *Mol. Phys.* **96**, 1391–1397.
107. Andrienko D., G. Germano, M. P. Allen (2000): ‘Liquid crystal director fluctuations and surface anchoring by molecular simulation’. *Phys. Rev. E* **62**, 6688–6693.
108. Bates M. A. , C. Zannoni (1997): ‘A molecular dynamics simulation study of the nematic-isotropic interface of a Gay-Berne liquid crystal’. *Chem. Phys. Lett.* **280**, 40–45.
109. Allen M. P. (2000): ‘Molecular simulation and theory of the isotropic-nematic interface’. *J. Chem. Phys.* **112**, 5447–5453.
110. Al-Barwani M. S., M. P. Allen (2000) ‘Isotropic-nematic interface of soft spherocylinders’. *Phys. Rev. E* **62**, 6706–6710.
111. McDonald A. J., M. P. Allen, F. Schmid (2001): ‘Surface tension of the isotropic-nematic interface’. *Phys. Rev. E* **63**, 10701–10704.
112. Akino N., F. Schmid, M. P. Allen (2001): ‘Molecular-dynamics study of the nematic-isotropic interface’. *Phys. Rev. E* **63**, 41706–41713.
113. Wall G. D. , D. J. Cleaver (1997): ‘Computer simulation studies of confined liquid-crystal films’. *Phys. Rev. E* **56**, 4306–4316.
114. Mills S. J., C. M. Care, M. P. Neal, D. J. Cleaver (1998): ‘Computer simulation of an unconfined liquid crystal film’. *Phys. Rev. E* **58**, 3284–3294.
115. Gruhn T., M. Schön (1998): ‘Substrate-induced order in confined nematic liquid-crystal films’. *J. Chem. Phys.* **108**, 9124–9136. *J CHEM PHYS* 108: (21) 9124-9136 JUN 1 1998
116. Gruhn T., M. Schön (1998): ‘Grand canonical ensemble Monte Carlo simulations of confined ‘nematic’ Gay-Berne films’. *Thin solid films* **330**, 46–58.
117. van Roij R., M. Dijkstra, R. Evans (2000): ‘Orientational wetting and capillary nematization of hard-rod fluids’. *Europhys. Lett.* **49**, 350–356.
118. Dijkstra M., R. van Roij, R. Evans (2001): ‘Wetting and capillary nematization of a hard-rod fluid: A simulation study’ *Phys. Rev. E* **63**, 051703–051710.

119. Allen M. P. (2000): 'Pressure tensor profiles at the isotropic-nematic interface'. Chem. Phys. Lett. **331**, 513–518.